ISSN 2706-6819 Vol.4, Issue 1: 1-6, DOI: 10.25236/IJFM.2022.040101

A Brief Review of Image Quality Assessment Techniques for Laparoscopic Image Restoration

Xiangwei Qin[1,2], Zhengyi Zhong[1,3], Hanze Wei[1], Rongrong Liu[1], Qun Wang[1*]

[1]Suzhou Institute of Biomedical Engineering and Technology, Chinese Academy of Sciences, Suzhou 215163, China
[2]School of Life Science and Technology, Changchun University of Science and Technology, Changchun 130022, China
[3]School of Mechanical Engineering, University of Shanghai for Science and Technology, Shanghai 200093, China
**Corresponding author*

Abstract: *Laparoscopic images usually suffer image degradation due to smoking, insufficient illumination, specularity, and limited fields of view. Computer-assisted restoration algorithms have been developed to tackle this problem, whose performance needs to be assessed through a mechanism of image quality evaluation. In this study, we will briefly exam several image quality assessment technologies that have been utilized in the process of laparoscopic image restoration.*

Keywords: *Image quality assessment, Non-Reference IQA, Full-Reference IQA, Laparoscopic images*

1. Introduction to Laparoscopic Image Quality Assessment

Laparoscopic images usually suffer deterioration from specularity, insufficient illuminations, smoking, and limited fields of view. This phenomenon is termed image degradation. Various computer-assisted interventions have been developed to address this issue by restoring image quality to its original state, a process known as image restoration.

Researchers developed a wide range of techniques known as Image Quality Assessment (IQA) to evaluate the performance of restoration algorithms, including subjective and objective evaluation. The subjective evaluation method employs humans to conduct an individual-based image assessment, similar to those used in psychology or sociology. The objective evaluation method's goal is to develop a computer algorithm for investigating image quality that is based on fundamental principles of digital image processing.

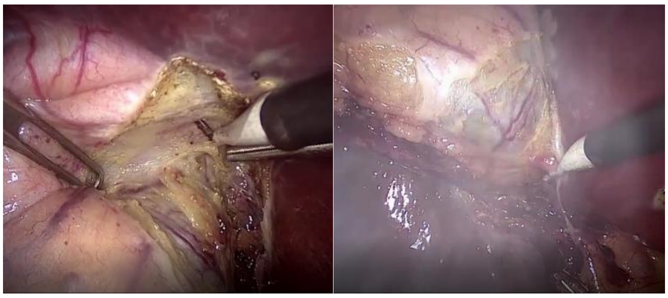

(a) *(b)*

Figure 1: Clean laparoscopic image (a) and deteriorated image (b) selected from dataset Cholec80 [1].

2. Introduction to Image Quality Assessment

Image Quality Assessment (IQAs), a subcategory objective evaluation, aims to construct computational models that can achieve reliable automation and accurate image quality prediction. The projected scores should be close to the average human observer in various settings and distortion types.

There are three different types of IQAs, Full-Reference IQA (FR-IQA), Reduce-Reference IQA

ISSN 2706-6819 Vol.4, Issue 1: 1-6, DOI: 10.25236/IJFM.2022.040101

(RR-IQA), and Non-Reference IQA (NR-IQA). FR-IQA requires all information of the reference image for one-to-one comparison and scoring at the pixel value level, which provides good accuracy. However, the reference image is difficult to obtain; NR-IQA analyzes image quality directly through the algorithm, which is more flexible in applications. For comparison and scoring, RR-IQA requires some statistical properties of the reference image, which has the advantage of requiring a limited quantity of data in practical applications.

In the study of laparoscopic image restoration, researchers developed numerous image evaluation approaches. This paper will not be able to cover all of these strategies. As a result, we've selected a number of representative samples of methods to highlight. In the following sections, we will review several Full-Reference methods and Non-Reference methods that have been mentioned in the research of laparoscopic image assessment in recent years.

3. Taxonomy of IQAs

3.1. FR-IQA

To assess the laparoscopic images, Full-Reference techniques are used to measure the difference between the referred image and the degraded image. FR-IQA compares the quality of the distorted image to the original, which is thought to be an undistorted version of the same image. The deviation of the distorted image from the reference image is used to calculate the amount of distortion.

As can be seen, the authors of [5-9] utilize NR-IQA algorithms to evaluate the efficacy of the degradation recovery system in their research. Some of the applied methods are listed below.

3.1.1. Mean Square Error (MSE)

Mean square error is calculated between the degraded image and the input image. It is computed by the following equation.

$$\mathrm{MSE} = \frac{1}{\mathrm{MN}} \sum_{1}^{\mathrm{M}-1} \sum_{1}^{\mathrm{N}-1} ((\mathrm{C}(\mathrm{x},\mathrm{y}) - (\mathrm{C}^{*}(\mathrm{x},\mathrm{y}))^{2}) \tag{1}$$

Here M and N are the apex and broadness of the input image. $C(x,y)$ and $C^{*}(x,y)$ are restored image and original image. The higher the value of MSE, the lower quality of the image is obtained.

3.1.2. Peak Signal-to-Noise Ratio (PSNR)

PSNR is calculated with respect to the input image and hazy image. It is given by

$$\mathrm{PSNR} = 10\log(255^{2}/\mathrm{MSE}) \tag{2}$$

The higher the value of PSNR, the better the image quality is.

3.1.3. Structural Similarity Index Measure

The drawback of MSE and PSNR is that only pixel-to-pixel variability is calculated, not accounting for human eyes' subjective perception of image quality. As a result, researchers proposed a novel method called Structural Similarity Index Measure (SSIM) [17], which measures the structural similarity between the reference image and the degraded image. It is inspired by the fact that the core functionality of human eyes is to extract structural information in the Field-of-View (FOV) and are highly adaptive to changes in the structure of the signal in the FOV.

SSIM is a perceptual image similarity metric that was proposed to increase the correlation with subjective evaluation. It is defined as:

$$SSIM(x,y) = (l(x,y))^{\alpha}(c(x,y))^{\beta}(s(x,y))^{\gamma} \tag{3}$$

In which $\mathrm{l}(\mathrm{x},\mathrm{y}) = \frac{2\mu_{\mathrm{A}}\mu_{\mathrm{B}}+\mathrm{C}_1}{\mu_{\mathrm{A}}^2+\mu_{\mathrm{B}}^2+\mathrm{C}_1}$, $\mathrm{c}(\mathrm{x},\mathrm{y}) = \frac{2\sigma_{\mathrm{A}}\sigma_{\mathrm{B}}+\mathrm{C}_2}{\sigma_{\mathrm{A}}^2+\sigma_{\mathrm{B}}^2+\mathrm{C}_2}$, $\mathrm{s}(\mathrm{x},\mathrm{y}) = \frac{\sigma_{\mathrm{AB}}+\mathrm{C}_3}{\sigma_{\mathrm{A}}\sigma_{\mathrm{B}}+\mathrm{C}_3}$, the simplified version of equation (3) proposed by Wang [17]

$$SSIM(x,y) = \frac{(2\mu_A\mu_B+C_1)(2\sigma_{AB}+C_2)}{(\mu_A^2+\mu_B^2+C_1)(\sigma_A^2+\sigma_B^2+C_2)} \tag{4}$$

Where μ_{A}, μ_{B} and $\mu_{\mathrm{AB}}$are mean and variance of images A and B correspondingly, while σ_{AB} is the covariance of the images.

ISSN 2706-6819 Vol.4, Issue 1: 1-6, DOI: 10.25236/IJFM.2022.040101

3.2. NR-IQA

Different from that of FR-IQA, NR-IQA algorithms provide the quality assessment of a laparoscopic image without a reference image or its features. Due to the absence of a reference image, one needs to build statistical models of the reference laparoscopic image, the effect of distortions, and the nature of the human visual system without supervision.

Researchers employed different NR-IQA methodologies to evaluate the quality of the recovered images in their studies [10-16]. Table 1 presents various assessment techniques that have been utilized in the process of image evaluation in terms of laparoscopic images analysis, as well as the comparison between these IQAs. We will review several of these methods in representative ways.

3.2.1. Natural Scene Statistics (NSS)

Natural Scene Statistics refers to the distribution of pixel intensities of natural images that deviate from distorted images. Pixel intensities of natural images follow a Gaussian Distribution after normalization, while unnatural or distorted ones do not. This difference in distributions is much more noticeable when we normalize pixel intensities and compute the distribution over these normalized intensities. Therefore, the deviation of the distribution from an ideal bell curve could measure the amount of distortion in the image.

3.2.2. Blind/Referenceless Image Spatial Quality Evaluator (BRISQUE)

BRISQUE is an NR-IQA method that employs four phases sequentially, which are extracting NSS, constructing feature vectors, and predicting using SVR. A. Mittal et al. [19] proposed the technique 2012. BRISQUE is statistically better than PSNR and SSIM and is highly competitive for all present-day distortion-generic NR-IQA algorithms. Not only that, low computational complexity makes it well suited for real-time applications.

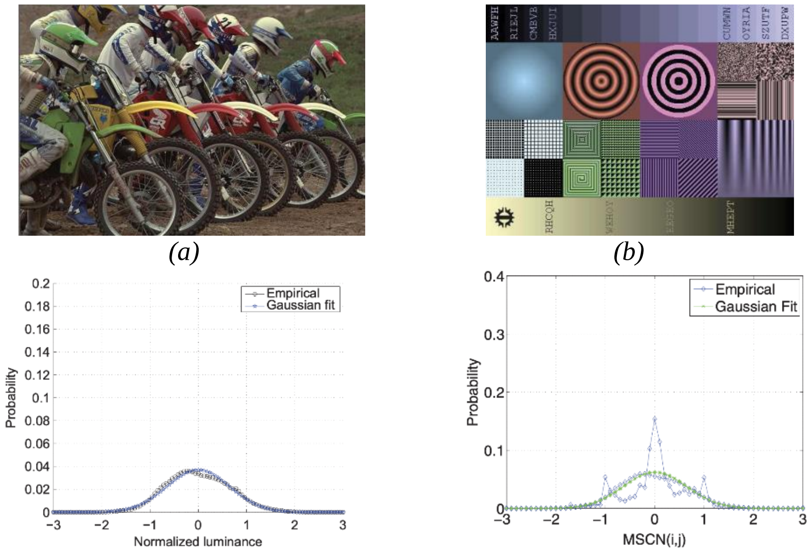

Figure 2: Natural image v.s. artificial image in terms of Gaussianity. (a) natural image, (b) artificial image, (c) Normalized luminance coefficients follow a nearly Gaussian distribution for (a), (d) the characteristic described in (c) does not hold true for the empirical distribution of (b)

3.2.3. Contrast-Changed Image Quality Assessment (CEIQA)

CEIQA assesses the quality of contrast changed images using histogram equalization from two aspects: image similarity and histogram-based entropy and cross-entropy. It constructs a framework that uses SSIM as the first feature to calculate the similarity of the original and augmented images. It starts by equalizing the histograms to create a better result, then computing the histogram-based entropy and cross-entropy between the original and enhanced ones. Finally, it learns to use a regression module to combine the five previously shown features to calculate the quality score.

ISSN 2706-6819 Vol.4, Issue 1: 1-6, DOI: 10.25236/IJFM.2022.040101

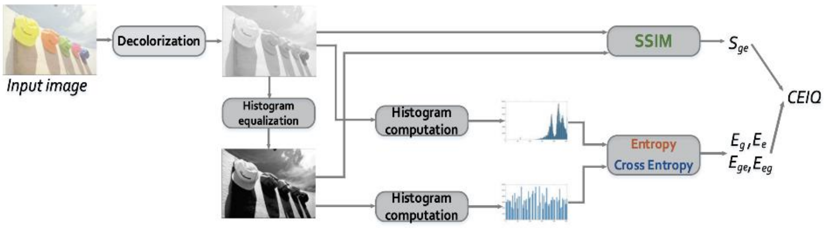

Figure 3: Feature extraction flowchart of CEIAQ [18].

3.2.4. Natural Image Quality Evaluator (NIQE)

Natural Image Quality Evaluator (NIQE) [22] is an image quality metric based on the NSS model in the spatial domain. In this method, the image is first subjected to local mean removal and divisive normalization, followed by calculating the local mean deviation. The distance of the Gaussian curve of NSS features of test images to natural images estimates image quality.

3.2.5. Just Noticeable Blur Metric (JNBM)

The human visual system (HVS) has a critical blur threshold during the detection of edge blur, which is called Just Noticeable Blur (JNB) [21]. While the blur recognition degree of HVS is subjective, the objective blur thresholds JNBs are determined by the local contrast. The JNB is the minimum value corresponding to the perceived blurring of the local edges of the image, provided that it is higher than the JND contrast. The Just Noticeable Difference (JND) is the minimum stimulus intensity value that can change sensory experience given the relative background intensity. The minimum contrast enables a standard observer to detect a change in intensity.

In the process of calculating JNB, the width and contrast of edge pixels are estimated to give the blur probability of that pixel; in addition, the blur evaluation of HVS is approximated using salient edge pixels; finally, the Cumulative Probability of Blur Detection (CPBD) is used to obtain the blur quality score.

4. Conclusion

Making assessments of degraded laparoscopic images is a challenging task. Researchers have developed various computational models to tackle this issue, categorized as FR-IQA and NR-IQA. We briefly reviewed some of the most popular techniques in this area and compared them to provide a clear picture of this research area.

Acknowledgements

This work is supported by National Key R&D Program of China, 2019YFC0118004

References

[1] A. P. Twinanda, S. Shehata, D. Mutter, J. Marescaux, M. de Mathelin and N. Padoy, "EndoNet: A Deep Architecture for Recognition Tasks on Laparoscopic Videos," in IEEE Transactions on Medical Imaging, vol. 36, no. 1, pp. 86-97, Jan. 2017.
[2] B. Li, X. Peng, Z. Wang, J. Xu, and D. Feng, "AOD-Net: All-in-One Dehazing Network," In Proceedings of IEEE International Conference on Computer Vision (ICCV), 2017.
[3] V. Venkatesh, N. Sharma, V. Srivastava, M. Singh, "Unsupervised smoke to desmoked laparoscopic surgery images using contrast driven Cyclic-DesmokeGAN," Computers in Biology and Medicine, Volume 123, 2020.
[4] J. Ho, S. Ermon, "Generative Adversarial Imitation Learning," Advances in Neural Information Processing Systems. 29: 4565-C4573, 2016.
[5] S. Salazar-Colores, H. M. Jiménez, C. J. Ortiz-Echeverri, and G. Flores, "Desmoking Laparoscopy Surgery Images Using an Image-to-Image Translation Guided by an Embedded Dark Channel," in IEEE Access, *vol. 8, pp. 208898-208909, 2020*
[6] M. A. Azam, K. B. Khan, E. Rehman et al, "Smoke Removal and Image Enhancement of Laparoscopic Images by An Artificial Multi-Exposure Image Fusion Method," 26 October 2021.
[7] Lin, J, Jiang, M, Pang, Y, et al. "A desmoking algorithm for endoscopic images based on improved

ISSN 2706-6819 Vol.4, Issue 1: 1-6, DOI: 10.25236/IJFM.2022.040101

U-Net model, " Concurrency Computat Pract Exper. 2021.
[8] S. Bolkar, C. Wang, F. A. Cheikh and S. Yildirim, "Deep Smoke Removal from Minimally Invasive Surgery Videos," 2018 25th IEEE International Conference on Image Processing (ICIP)*, 2018, pp. 3403-3407*
[9] C. Wang, A. Kedir Mohammed, F. Alaya Cheikh et al., "Multiscale deep desmoking for laparoscopic surgery," Proc. SPIE 10949, Medical Imaging 2019: Image Processing, 109491Y, 2019.
[10] Vishal V., Sharma N., Singh M. "Guided Unsupervised Desmoking of Laparoscopic Images Using Cycle-Desmoke". In: Zhou L. et al. (eds) OR 2.0 Context-Aware Operating Theaters and Machine Learning in Clinical Neuroimaging. OR 2.0 2019, MLCN 2019. Lecture Notes in Computer Science, vol 11796. Springer, Cham.
[11] K. He, J. Sun and X. O. Tang, "Single image haze removal using dark channel prior," 2009 IEEE Conference on Computer Vision and Pattern Recognition, 2009, pp. 1956-1963.
[12] A Odena, "Semi-supervised learning with generative adversarial networks Workshop on Data-Efficient Machine Learning", ICML 2016.
[13] K. S and M. Durgadevi, "Generative Adversarial Network (GAN): a general review on different variants of GAN and applications," 2021 6th International Conference on Communication and Electronics Systems (ICCES), 2021, pp. 1-8.
[14] A. Baid, A. Kotwal, R. Bhalodia, S. N. Merchant, and S. P. Awate, "Joint Desmoking, Specularity Removal, and Denoising of Laparoscopy Images Via Graphical Models and Bayesian Inference" Indian Institute of Technology (IIT) Bombay. University of Utah., in IEEE 14th International Symposium on Biomedical Imaging, 2017, pp. 732–736.
[15] A. Kotwal, "Joint Desmoking and Denoising of Laparoscopy Images" Department of Electrical Engineering Indian Institute of Technology (IIT) Bombay Department of Computer Science and Engineering Indian Institute of Technology (IIT) Bombay," in IEEE 13th International Symposium on Biomedical Imaging (ISBI), 2016, pp. 1050–1054.
[16] O. Sidorov, C. Wang, F. Alaya, "Generative Smoke Removal" Cheikh Proceedings of the Machine Learning for Health NeurIPS Workshop, PMLR 116:81-92, 2020.
[17] Z. Wang, A. C. Bovik, H. R. Sheikh, and E. P. Simoncelli, "Image Quality Assessment: from Error Visibility to Structural Similarity," IEEE Transactions on Image Processing 13, 4, 600–612, 2004.
[18] Yan, Jia, J. Li, and X. Fu 2019 No-Reference Quality Assessment of Contrast-Distorted Images using Contrast Enhancement 2019 arXiv abs/1904.08879 (Preprint 1904.08879)
[19] A. Mittal, A. K. Moorthy and A. C. Bovik, "No-Reference Image Quality Assessment in the Spatial Domain," in IEEE Transactions on Image Processing, vol. 21, no. 12, pp. 4695-4708, Dec. 2012.
[20] C. Wang, F. Alaya Cheikh, M. Kaaniche et al. "Variational based smoke removal in laparoscopic images," BioMed Eng OnLine 17, 139, 2018.
[21] R. Ferzli and L. J. Karam, "A No-Reference Objective Image Sharpness Metric Based on the Notion of Just Noticeable Blur (JNB)," in IEEE Transactions on Image Processing, vol. 18, no. 4, pp. 717-728, April 2009.
[22] A. Mittal, R. Soundararajan and A. C. Bovik, "Making a Completely Blind Image Quality Analyzer," IEEE Signal processing Letters, pp. 209-212, vol. 22, no. 3, March 2013.

ISSN 2706-6819 Vol.4, Issue 1: 1-6, DOI: 10.25236/IJFM.2022.040101

Table 1: Comparison between different IQAs

	PSNR	SSIM	FSIM	UQI	BRISQE	PIQUE	CEIQ	NIQE	FADE	Blur	JNBM	Edge	RE	MICM	RRMSE	Subjective
[5]	√	√	√	√												
[10]					√	√	√									
[16]																√
[2]	√	√														
[7]	√	√														
[3]							√	√	√							
[6]									√	√	√	√				
[20]									√		√		√	√		
[15]															√	√
[9]	√	√														